CENTRAL COMPOSITE DESIGN (CCD) USING RESPONSE SURFACE METHODOLOGY OF LOCALLY-PRODUCED-XYLOSE-REDUCTASE PURIFICATION BY REVERSE MICELLE

Rusmawarni Ramli[1], Nurul Iman Abd Razak[2]

[1]*Instrumentation and Control Engineering Section, Universiti Kuala Lumpur, Malaysian Institute of Industrial Technology, Jalan Persiaran Sinar Ilmu, 81750, Bandar Seri Alam, Masai, Johor*

[2]*School of Chemical and Energy, Faculty of Engineering, Universiti Teknologi Malaysia, 81310, Skudai, Johor*

Corresponding Author: rusmawarni@unikl.edu.my

ABSTRACT

Enzyme purification is one of the essential methods in this study since the availability of the reusable enzyme is needed. Mathematical modeling used in this study was response surface methodology (RSM) and the tool used was the design of expert (DOE) software. The aim of using the tools was to optimize the significance of variables involved in the enzyme purification process for enhancing the capability of enzyme recovery. The OFAT of enzyme purification was conducted under the concentration of surfactant (2.3% – 2.7%), range of pH (4.5 - 6.5), and concentration of salt, M (0.75 – 1.50). Further optimization by RSM was followed, and at the end, the optimum variables were the concentration of surfactant at 2.70%, pH at 6.48, and salt concentration at 0.8443M. The validation was repeated for the significant variables. The percentage error of the predicted vs. the actual value was only 0.91% which means the study of the enzyme purification by significance variables chose can be accepted.

Keywords: *Bio-separation, Design Expert 11, PAGE-electrophoresis, UV-Vis, central composite design (CCD).*

1. INTRODUCTION

Recently, advances in biotechnology have opened up numerous possibilities for the purification of many biomolecules that are important for research, pharmaceuticals, and other industrial applications. The research and development of techniques and methods for separating and purification of enzymes and other biomolecules have been of paramount importance for many of these biotechnology industries' advances. The traditional methods to purify biomolecules involve several steps, such as dialysis, ionic and affinity chromatography, and others from the previous methodologies that have been done. However, liquid-liquid extractions are an exciting purification alternative since several early processing steps can be combined into a single operation. Liquid-liquid extraction transfers specific components from one phase to another when immiscible or partially soluble liquid phases contact each other.

Liquid-liquid extraction by reversed micelles is a valuable and versatile tool for separating biomolecules. This process shows a close similarity to the traditional liquid-liquid extraction process. Both are biphasic and consist of partitioning a target solute between an aqueous phase and an organic phase, with subsequent back transfer second aqueous stripping phase [1]. This method involves using ternary mixtures composed of water-surfactant-solvent, a first step (forward extraction). Through agitation, this leads to the aggregation of surfactant molecules that form a hydrophilic core (reverse micelles) where the enzyme to be purified can be integrated. In a second step (backward extraction), through its transfer to a new aqueous phase, the reverse micelles' enzyme is released to observe the quantitative recovery of purified protein [2].

This process is widely employed in the chemical industry due to its simplicity, low costs, and ease of scale. Purification of biomolecules using liquid-liquid extraction has been successfully carried out on a large scale for more than a decade. The advantages of using this system are lower viscosity, lower cost of chemicals, and shorter phase separation time. These systems' dynamic behavior must be investigated and understood to enhance plant-wide control of continuous liquid-liquid extraction and assess the safety and environmental risks at the earliest possible design stage. Reversed micellar extraction is an innovative method for separating and purifying proteins and other biomolecules. The surfactant molecules assemble themselves with the polar head to the inner side and the polar tail in contact with the organic solvent. Reverse micellar extraction has attracted much attention for its energy-saving feature and the possibility of sequential operations.

2. MATERIALS AND METHODS

Preparation of locally-produced Xylose reductase (LPXR)

LPXR has been extracted from meranti wood sawdust hydrolysate (MWSH). Meranti wood sawdust (MWS) was purchased from a nearby sawmill with the bulk sampling. The MWS were soaked and washed with hot water until the filtered water became clear water. The purpose of this process is to remove the foreign particles and machine oil from the sawmill. The MWS then dried in the oven at 105ºC for 24 hours or constant moisture content. Equation 1 was used to calculate the moisture content of the MWS [4].

$$Mass\ (dry\ basis) = \frac{|w-d|}{d} \times 100, \quad (1)$$

where:

w = wet weight of the leaves

d = dry weight of the leaves at a specific temperature.

The washed MWS then treated using 2.0% of Sulfuric acid for 120 minutes at 80ºC to eliminate the lignin content in the MWS. The treated MWS will be used in the extraction of LPXR. The liquor-treated MWS named MWSH. The MWSH will proceed with the extraction process using an ultrasonic probe at 20KHz for 30 minutes in a cold condition. Figure 1 below shows the extraction of LPXR from MSWH. The liquor from the extraction process will be kept in the freezer at -20ºC for further use.

Figure 1: The extraction process of locally-produced xylose reductase from MWSH

Preparation of Micellar Solution and Purification of LPXR using Reverse Micelle

Forward extraction of LPXR was typically carried out by mixing MWSH preparation in isooctane in the presence of surfactant under constant stirring conditions at stated temperature and time. Surfactants used in this work are AOT, CTAB, SDS, and Triton X-100 were added. All surfactants except AOT were directly added to crude LPXR preparation while AOT was first dissolved in isooctane. Effect of different surfactants, different concentrations of CTAB as surfactants (2.3% to 2.7%), range of pH (4.5 to 6.5), and concentration of salt (1.75 to 1.50) were studied. The forward extraction containing micro-emulsion was incubated at stated temperatures and stated time with constant stirring. The reaction mixture was then centrifuged at 8000g for 10 min at 25^{o}C. The two phases (aqueous and organic) were separated, and the residual activity of LPXR was checked in the aqueous phase [1].

Qualitative Analysis by SDS-PAGE

SDS-PAGE was used to indicate the activity of the LPXR or enzyme.

Quantitative analysis by UV-Vis

The sugar/xylose produce from the activity of the LPXR was analyze using UV-Vis at 671 nm. The xylose standard was purchased from Merck Malaysia with a 95% of analytical grade.

Design of experiment by a design expert, version 11

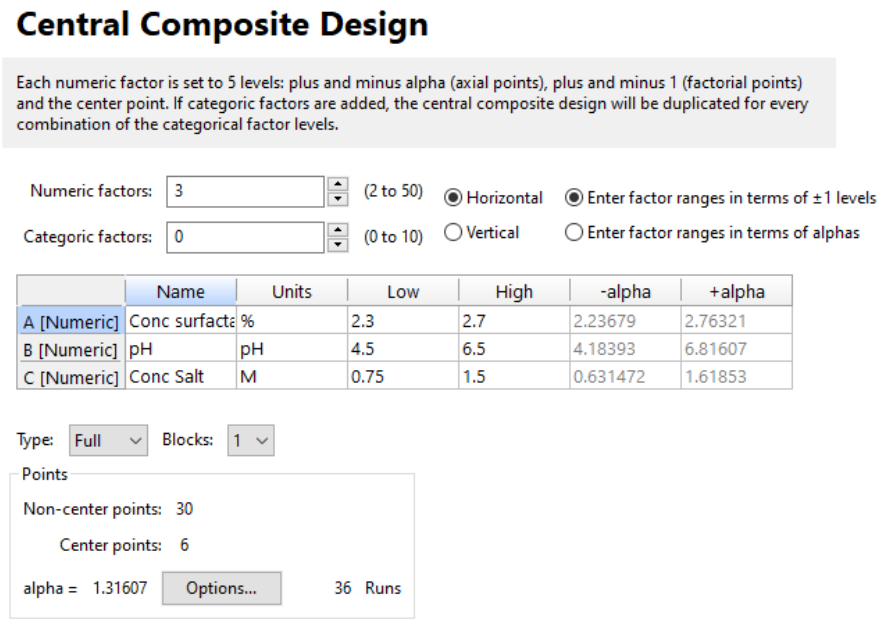

Figure 2: Set up of the experiment for enzyme purification by reverse micelle

Table 1: Number of experiment design using design expert software, version 11

Run	Concentration of surfactant (%)	pH	Concentration of Salt (M)	Concentration of Xylose (mg/L)
1	2.50	5.50	1.13	
2	2.50	5.50	1.13	
3	2.30	6.50	1.50	

4	2.30	4.50	0.75
5	2.50	4.18	1.13
6	2.50	5.50	0.63
7	2.70	6.50	1.50
8	2.30	4.50	0.75
9	2.24	5.50	1.13
10	2.30	4.50	1.50
11	2.70	4.50	1.50
12	2.70	4.50	0.75
13	2.30	6.50	1.50
14	2.70	6.50	1.50
15	2.76	5.50	1.13
16	2.70	4.50	1.50
17	2.50	5.50	1.13
18	2.50	5.50	1.13
19	2.50	5.50	1.13
20	2.30	6.50	0.75
21	2.30	4.50	1.50
22	2.70	4.50	0.75
23	2.30	4.50	0.75
24	2.30	6.50	0.75
25	2.70	4.50	1.50
26	2.50	5.50	1.13
27	2.50	5.50	1.62
28	2.70	6.50	0.75
29	2.70	6.50	1.50
30	2.70	6.50	0.75
31	2.30	6.50	0.75
32	2.70	6.50	0.75
33	2.70	4.50	0.75
34	2.50	6.82	1.13
35	2.30	6.50	1.50
36	2.30	4.50	1.50

3. RESULT AND DISCUSSION

Characteristic of Meranti wood sawdust using FTIR Spectrometry

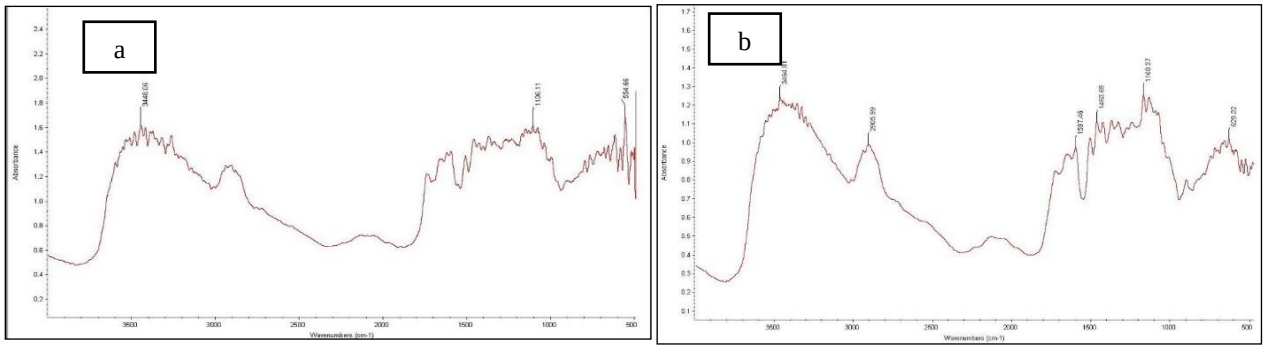

Figure 3a: FTIR spectrum for Meranti wood sawdust (untreated)
Figure 3b: FTIR spectrum for Meranti wood sawdust (after treated with 2.0% of Sulfuric Acid)

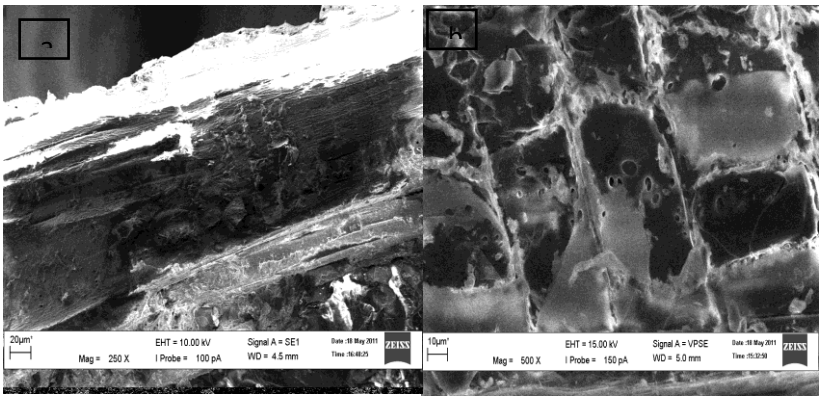

Figure 4: SEM image for meranti wood sawdust (untreated)

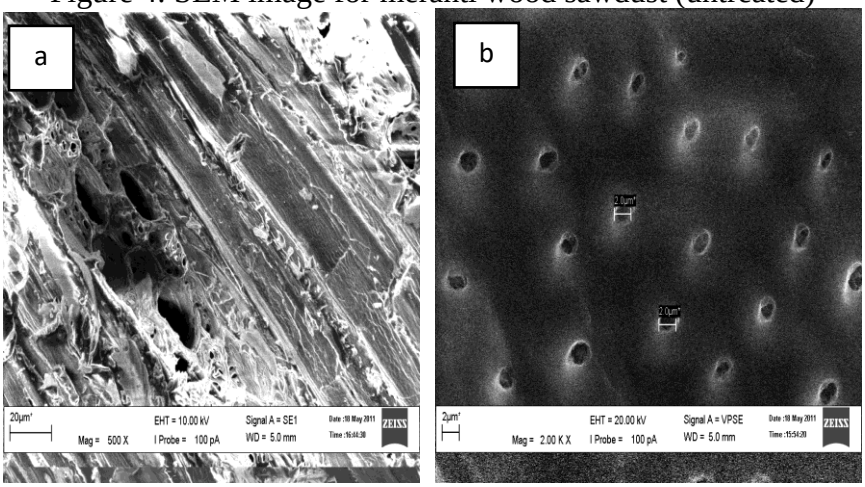

Figure 5: SEM image for meranti wood sawdust (after treated with 2.0% of Sulfuric Acid)

Figures 2,3, 4, and 5, the difference between the sawdust before and after treatment is proof well. The structure of the MSW has more pores compared to the untreated. This characteristic will give a good interaction and reaction between the MSW and the surfactant to separate and purify the enzyme produced. The standard curve shown in Figure 6 was used to calculate the xylose content produced. This concentration of the xylose was indicated the purification of the LPXR success.

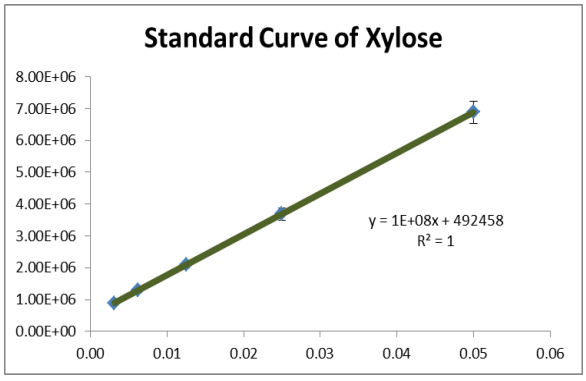

Figure 6: Standard curve of xylose from calibration procedure.

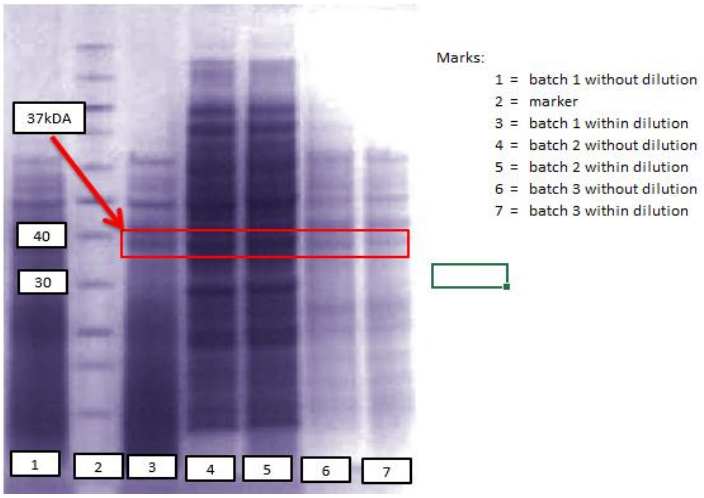

Figure 7: Image of SDS-PAGE for enzyme purification using Reverse Micelle method.

Figure 7 shows the result of the SDS-PAGE for analyzing the enzyme present in the MWSH. Based on Yokohama, 2019, the xylose reductase or any locally-produced xylose reductase appeared at 37-40 kDa.

Analysis of Variance (ANOVA) for locally-produced Xylose reductase

Table 2: The Analysis of Variance (ANOVA) of the purification process

Source	Sum of squares	df	Mean square	F-value	P-value	
Model	2048.9425	9	227.66028	40.61633	6.519E-11	*a
A-Conc surfactant	1046.3413	1	1046.3413	186.67528	1.329E-11	
B-pH	49.859738	1	49.859738	8.8953576	0.0073599	
C-Conc Salt	408.90334	1	408.90334	72.951475	4.179E-08	
AB	934.50052	1	934.50052	166.72202	3.686E-11	
AC	310.40209	1	310.40209	55.3781	3.499E-07	
BC	156.30344	1	156.30344	27.885726	3.618E-05	
A^2	305.06179	1	305.06179	54.425351	3.982E-07	
B^2	3.3821488	1	3.3821488	0.6034012	0.4463739	
C^2	80.607818	1	80.607818	14.38105	0.001143	
Residual	112.10283	20	5.6051415			
Lack of Fit	25.105947	2	12.552973	2.5972599	0.1020902	*b
Pure Error	86.996883	18	4.8331602			
Cor Total	2161.0453	29				

*a = significant
*b = not significant

The Model F-value of 40.62 implies the model is significant. There is only a 0.01% chance that an F-value this large could occur due to noise. P-values less than 0.0500 indicate model terms are significant. In this case, A, B, C, AB, AC, BC, A^2, C^2 are significant model terms. Values greater than 0.1000 indicate the model terms are not significant. If there are many insignificant model terms (not counting those required to support hierarchy), model reduction may improve

your model. The Lack of Fit F-value of 2.60 implies the Lack of Fit is not significant relative to the pure error. There is a 10.21% chance that a Lack of Fit F-value this large could occur due to noise. The non-significant lack of fit is good, and the model is excellent. In this case, the model did not proceed with the model reduction since the value of the R-squared was good enough. The R-squared value was more than 95% if it is referring to theTable 3. The adjusted R-squared is still more than 90% and indicates the model is good enough and does not need to come out with the model reduction.

Table 3: R-squared value for the ANOVA model

Std. Dev.	2.367518	R^2	0.9481256
Mean	107.54416	Adjusted R^2	0.9247822
		Predicted	
C.V. %	2.201438	R^2	0.8346837
		Adeq Precision	19.837402

The Predicted R^2 of 0.8347 is in reasonable agreement with the Adjusted R^2 of 0.9248; i.e., the difference is less than 0.2. Adequate Precision measures the signal-to-noise ratio. Hence, the ratio was more significant than four, and it is desirable. The model ratio of 19.837 indicates an adequate signal. This model can be used to navigate the design space. At the same time, the actual equation will use for further data analysis and interacting part.

Table 4: Coded equation vs. actual equation

Coded		Actual	
Concentration Xylose	=	Concentration Xylose	=
102.0237		2011.4197	
9.1597	A	-1332.8611	Conc surfactant
-1.8530	B	-93.9163	pH
-5.6758	C	-51.0023	Conc Salt
8.8685	AB	44.3424	Conc surfactant * pH
4.9094	AC	65.4584	Conc surfactant * Conc Salt
-3.4838	BC	-9.2900	pH * Conc Salt
8.4891	A^2	212.2272	Conc surfactant^2
-0.7583	B^2	-0.7583	pH^2
-4.7927	C^2	-34.0817	Conc Salt^2

The equation in terms of coded factors can be used to make predictions about the response for given levels of each element. By default, the high levels of the factors are coded as +1, and the low levels are coded as -1. The coded equation helps identify the relative impact of the factors by comparing the factor coefficients. The equation in terms of fundamental factors can be used to make predictions about the response for given levels of each factor. Here, the levels should be specified in the original units for each factor. This equation should not be used to determine the

relative impact of each factor because the coefficients are scaled to accommodate the units of each factor, and the intercept is not at the center of the design space [3].

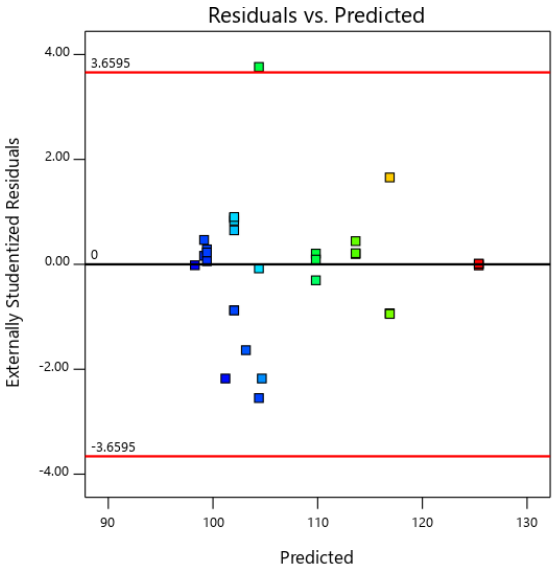

Figure 8: The Residual vs. Predicted graph.

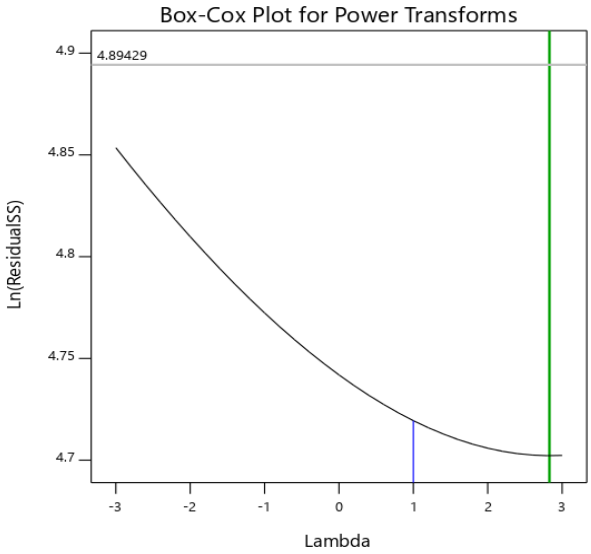

Figure 9: Box-cox Plot for power transforms of the model.

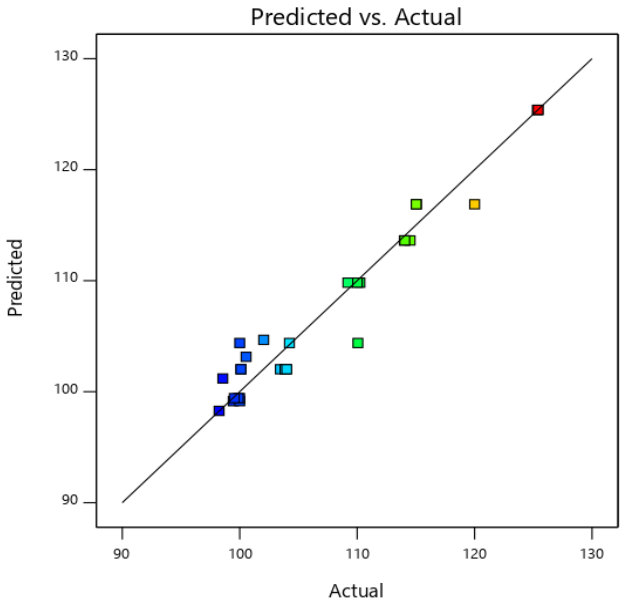

Figure 10: The Predicted vs. Actual graph for the model chosen.

Figures 8, 9, and 10 show the tabulated data for the model choose. The graph shows the data is well balanced, and six data were neglected due to the imbalance of the results. The rows of the data were experiment run numbers 24, 13, 35, 3, 15, and 27. Meanwhile, Figures 11, 12, and 13 show the interaction of the factors towards the LPXR purification and xylose concentration as an indicator for the purification process [5]. The graph shows the interactions of the three factors that were excellent to design the model. The 3D model of each interaction shows every factor needs each other.

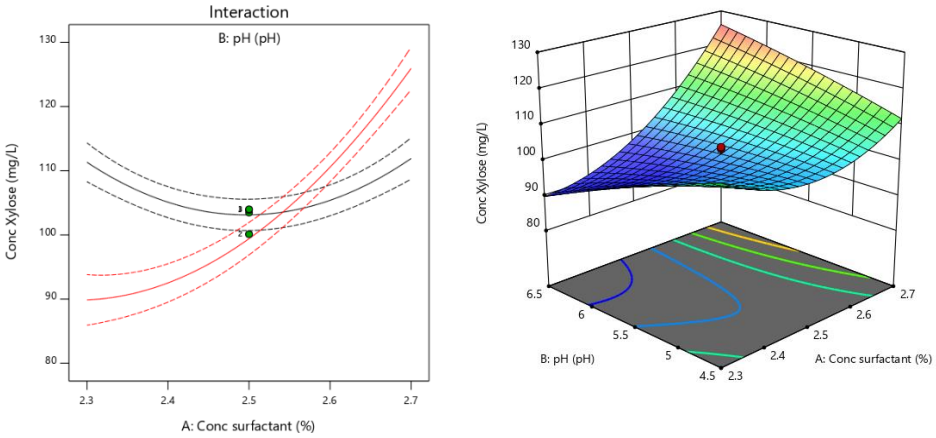

Figure 11: The Interaction between the Concentration of surfactant and pH towards xylose concentration as an indicator of the LPXR purification.

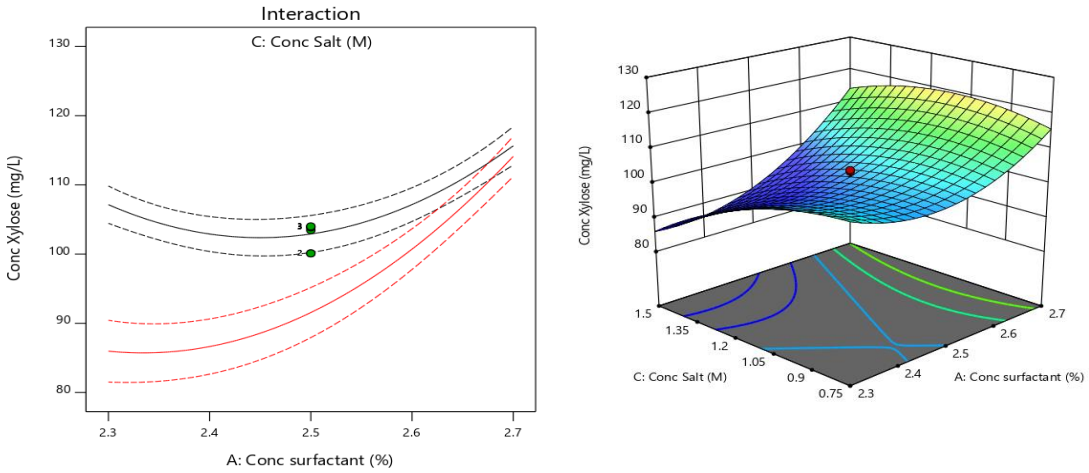

Figure 12: The Interaction between the Concentration of surfactant and concentration of salt towards xylose concentration as an indicator of the LPXR purification.

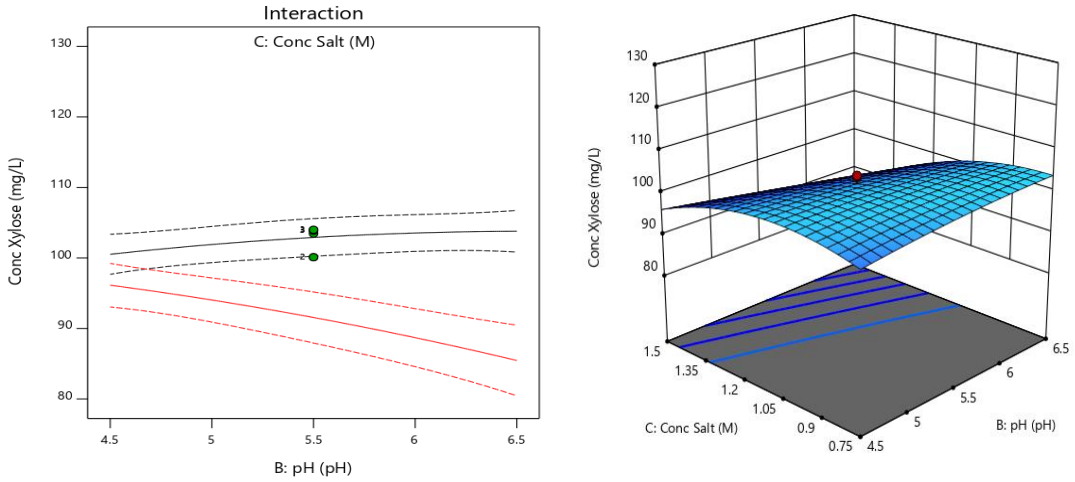

Figure 13: The Interaction between Concentration of salt (M) and pH towards xylose concentration as an indicator of the LPXR purification.

Optimization of model for locally-produced Xylose reductase

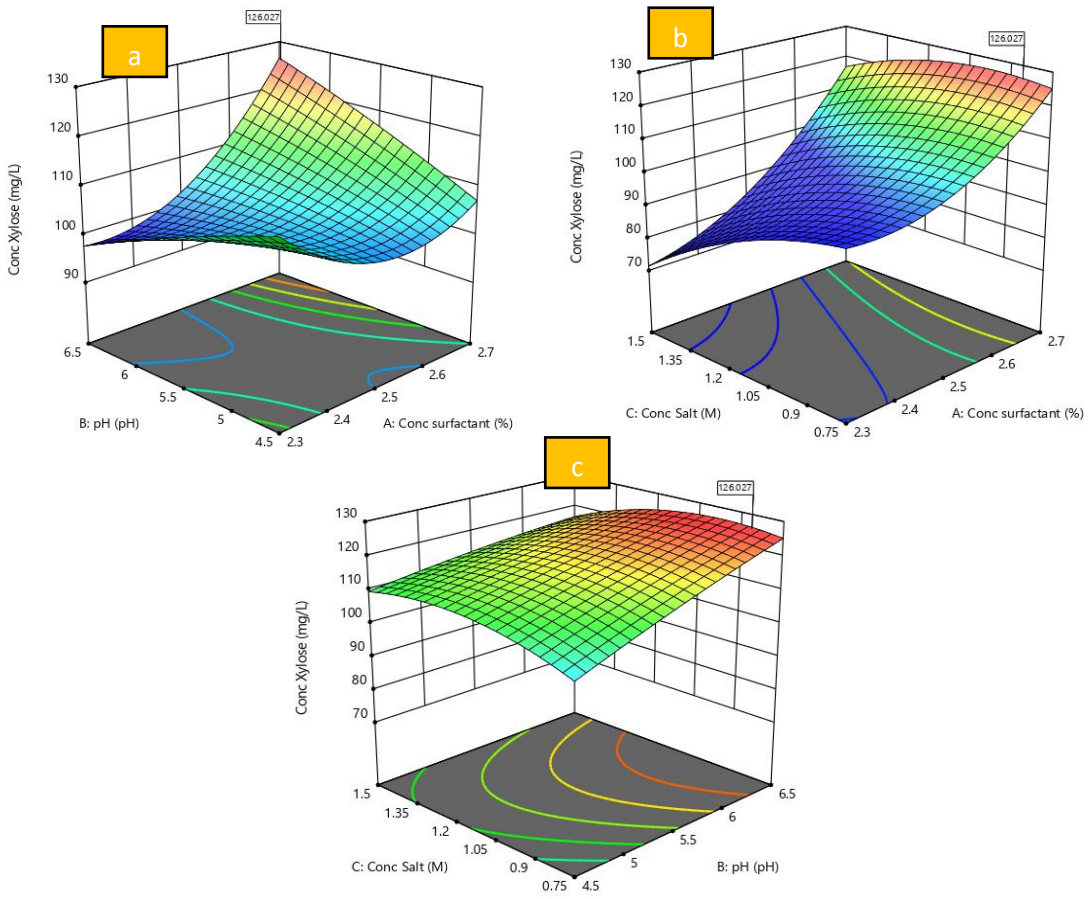

Figure 14: 3D model of optimization for LPXR purification (xylose concentration as an indicator

Figures 14a, 14b, and 14c show the model of optimization study for three factors; pH, the concentration of surfactant(%), and the concentration of salt (M) [4]. The 3D graph gave an excellent understanding which the maximum xylose concentration produced for this hydrolysis done by LPXR was 126.027 mg/L. Meanwhile, the suit condition of the factors to produce 126.027 mg/L xylose were at 2.7% of surfactant concentration, pH 6.48, and 0.8443 M of salt concentration.

Validation of a model for locally-produced Xylose reductase

Table 4 was validation data for the predicted value and actual value of each factors pairs suggested by the software. The average is only 0.99% from the percentage error, which means the predicted values suggested by the model were acceptable.

Table 4: The validation of the model for the purification process of LPXR

The concentration of surfactant (%)	**pH**	**The concentration of salt (M)**	**Predicted value**	**Actual value**	**% Error**
2.69	6.40	1.1000	125.5070	124.3440	**0.03**

2.70	6.47	1.0800	126.2240	125.9432	**0.22**
2.70	6.48	0.7900	125.4670	124.3341	**0.99**
2.70	6.45	1.0000	126.4431	123.4431	**2.38**

4. CONCLUSION

For the conclusion, the LPXR was extracted from the MSWH using the ultrasonic probe at the high frequency, 20kHz. The xylose concentration produced from the reaction of the MWSH with the LPXR indicates the enzyme activities during the purification process.

5. RECOMMENDATION

The one factor at a time (OFAT) study should be extended before continue with the central composite design(CCD) to enhance the range of each factor involved. This is needed since, from the model design, the range of the factors is too broad, and at the same time, a few factors are also too closed. This result will be affected by the predicted value suggested by the model.

6. REFERENCES

[1] Rawat, U. B. and Rao, M. B., (2016). Purification, kinetic characterization, and involvement of tryptophan residue at the NADPH binding site of xylose reductase from *Neurospora crassa*. *Biochimica et Biophysica Acta*. 1293: 222-230.

[2] Ronzon, Y. C., Zaldo, M. Z., Lozano, M. L. D. C. and Uscanga, M. A. (2018). Preliminary characterization of xylose reductase partially purified by reversed micelles from candida tropicalis IEC5-ITV, an indigenous xylitol-producing strain. *Advance in chemical engineering and science*. 2: 9-14.

[3] Rusmawarni Ramli (2020), Mathematical Modelling of Total Suspended Solid Removal From Pome Via Modified Electrocoagulation, Journal of Critical Reviews, Vol 7, Issue 8, 67-71, DOI: 10.31838/jcr.07.08.14

[4] Woodyer, R., Simurdiak, M., Donk, W. A. V., and Zhao, H. (2019). Heterologous Expression, purification, and characterization of a highly active xylose reductase from Neurospora crassa. *Applied and Environmental Microbiology*. 71: 1642-1647.

[5] Yokohama, S. I., Suzuki, T., Kawai, K., Horitsu, H. and Takamizawa, K. (2019). Purification, characterization, and structure analysis of NADPH-Dependent D-xylose reductase from Candida tropicalis. *Journal of fermentation and Bioengineering*. 79: 217-223.